Journal of Scientific & Industrial Research
Vol. 85, March 2026, pp. 244-251
DOI: 10.56042/jsir.v85i3.5762

Independent Features Outperform Uncorrelated Approaches in ML Classification

Rajesh Patel*, C. Kesavaraja & S. Sengottuvel

SQUIDs Applications Section, SQUIDs & Detector Technology Division, Materials Science Group,
Indira Gandhi Centre for Atomic Research, HBNI, Kalpakkam 603 102, India

Received 22 September 2023; revised 21 December 2024; accepted 06 February 2026

Prior EEG research has primarily focused on N-back cognitive task data, utilizing established techniques such as time-frequency spectrum and wavelet-based methods for feature extraction. However, Principal Component Analysis (PCA), despite its utility in boosting classifier performance, falls short in capturing nonlinear feature relationships. This study proposes a novel approach that integrates Multivariate Empirical Mode Decomposition (MEMD) with Independent Component Analysis (ICA) to enhance signal processing and feature extraction. Multivariate empirical mode decomposition generates analytic functions from EEG data by decomposing the multichannel EEG into Intrinsic Mode Functions (IMFs), from which diverse features are extracted. ICA then further reduces dimensionality, leveraging higher-order statistics to pinpoint critical features. The resulting significant, independent features are used to train and test various machine learning models, with the k-nearest neighbors algorithm emerging as the most successful, achieving a remarkable 95.27% classification accuracy. This approach enhances feature extraction and classification of cognitive task-related EEG data.

Keywords: Classification, Features extraction, Independent component analysis, Intrinsic mode functions**,** Multivariate empirical mode decomposition

Introduction

Human error remains a dominant contributor to industrial accidents, with operator cognitive overload among the most significant underlying causes.[1] As modern industrial environments become increasingly automated and complex, ensuring operator safety and system reliability requires continuous and objective monitoring of mental workload. Consequently, real-time assessment of operator functional states has emerged as a critical research focus in occupational safety and human-machine interaction studies. Among neurophysiological measurement modalities, electroencephalography (EEG) is widely employed for cognitive state assessment owing to its excellent temporal precision, non-invasive operation, and feasibility for real-time, portable monitoring.[2,3] Despite these advantages, practical analysis of EEG signals remains challenging because brain activity exhibits strong non-stationarity, non-linearity, and subject-specific variability during cognitive tasks. These characteristics limit the effectiveness of many conventional signal processing approaches currently adopted in the literature.

Most existing EEG-based workload assessment frameworks rely on classical time-frequency analysis techniques, including the Short-Time Fourier Transform (STFT) and wavelet-based methods.[4] Although these approaches have demonstrated success for quasi-stationary signals, their performance degrades when applied to EEG data due to their dependence on predefined basis functions, such as sinusoidal kernels or selected mother wavelets. This fixed-basis assumption constrains the representation of inherently adaptive neural oscillations and may obscure task-related dynamics. Moreover, identifying optimal analysis parameters often requires extensive empirical tuning, resulting in increased computational cost and limited generalizability across subjects and experimental conditions.[5] Beyond signal decomposition, feature dimensionality reduction poses another critical challenge. Principal Component Analysis (PCA) is commonly employed to reduce feature space; however, it is restricted to second-order statistics and primarily performs decorrelation rather than actual source separation. As a result, higher-order statistical dependencies, which are essential for discriminating independent neural processes, are neglected mainly.[7] Alternatively, kernel-based or higher-order polynomial methods can capture more complex relationships but typically incur substantial computational overhead, rendering them unsuitable for real-time or embedded implementations. These

*Author for Correspondence
E-mail: prajesh@igcar.gov.in

limitations highlight a clear research gap: the lack of adaptive, data-driven frameworks capable of addressing EEG non-stationarity while efficiently extracting higher-order independent features without reliance on manually defined priors or excessive computational complexity.

To address these challenges, this study proposes a fully data-driven signal analysis framework that integrates Multivariate Empirical Mode Decomposition (MEMD) with Independent Component Analysis (ICA). Multivariate empirical mode decomposition adaptively decomposes multichannel EEG signals into Intrinsic Mode Functions (IMFs) derived directly from the data, thereby avoiding the constraints imposed by fixed basis functions. Importantly, MEMD ensures mode alignment across channels, which is essential for meaningful interpretation of multichannel cognitive dynamics.[5,6] To further enhance feature representation; ICA is employed to extract statistically independent components based on higher-order statistics. Compared to PCA, ICA yields a more compact and discriminative feature space that better reflects underlying neural sources. The proposed MEMD–ICA framework is evaluated using EEG data acquired during an N-back cognitive workload task. Classification performance is validated using machine learning models, including the K-Nearest Neighbor classifier. The results demonstrate improved accuracy and computational efficiency, highlighting the framework's effectiveness for real-time analysis of non-stationary biomedical signals and its potential to overcome the limitations of conventional fixed-basis EEG processing techniques.

The workflow involved in the proposed approach for the N-back EEG task classification is illustrated in Fig. 1.

MEMD and ICA

MEMD

The extension of Empirical Mode Decomposition (EMD) is called MEMD, which allows the decomposition of multi-channel data.[8] Multivariate empirical mode decomposition (MEMD) decomposes multichannel data into intrinsic mode functions (IMFs), capturing multiple oscillatory modes. In MEMD, the sifting process is employed to extract successive IMFs, which must satisfy the following two conditions:

1 The mean of the upper and lower local envelopes, defined by the maxima and minima, must be zero.
2 The difference between the number of zero crossings and the number of extrema must not exceed one.

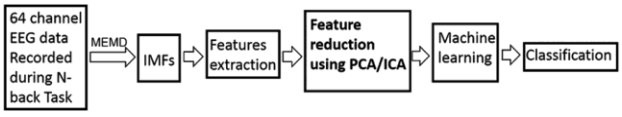

Fig. 1 — Block diagram illustrating the proposed approach used in the current study

In the process of MEMD, multiple envelopes are derived by projecting multichannel signals along various directions in an n-dimensional space. For a sequence of n-dimensional vectors s(t) = {s1(t), s2(t), ..., sn(t)}, which represent multivariate signal of n channels and xv = x^v_1, x^v_2, ..., x^v_n denoting a set v = 1, 2, ..., V direction vectors along the directions of the angles as $\theta_v = \theta_{v1}, \theta_{v2}, ..., \theta_{vn}$ in n space. The implementation of the MEMD algorithm involves the following steps:

i. Initiate by choosing an appropriate set of points for sampling an (n-1) sphere. Next, compute the corresponding projections $w_{\theta v}$ of the input signal s(t) onto the direction vectors x^v for v = 1, 2, ...V.
ii. Compute the time instants $t^i_{\theta v}$ corresponding to the peaks of the projected signals for v = 1, 2, ..., V.
iii. Interpolate the points $[t^i_{\theta v}, s(t^i_{\theta v})]$ to obtain the multivariate envelope curves $e^i_{\theta v}$ for v = 1, 2, ..., V.
iv. Calculate the mean of the V multidimensional envelopes.

$$m(t) = \frac{1}{v}\sum_{v=1}^{V} e_{\theta v}(t) \quad \ldots (1)$$

v. The mean is subtracted from the signal to obtain the detailed component, d(t) = s(t) − m(t). If the stoppage condition is met by d(t) for a multivariate IMF, apply the procedure as mentioned above to extract an IMF such as s(t) - d(t). Otherwise, iterate the process to compute a new d(t).

ICA

PCA is one of the popular techniques commonly used for data analysis and dimension reduction.[9] PCA projects the high-dimensional data onto a lower-dimensional subspace while preserving most of the information contained in the original dataset.[10] Assume the input data $\{x_i\}$, where i=1…n. The covariance matrix used in PCA is expressed as:

$$Cov = \frac{1}{n}\sum_{j=1}^{n}\left(\phi(X_j)\phi(X_j)^T\right) \quad \ldots (2)$$

where, n is the number of data points.

The corresponding eigen values can be calculated as

$$\lambda \vartheta = Cov\vartheta \quad \ldots (3)$$

where, λ denotes the eigenvalues and ϑ represents the corresponding eigenvectors in the feature space. PCA transforms the original data into linearly uncorrelated principal components. The significant principal components are calculated using the scree plot. Scree plot shows eigenvalues for each principal component, where the eigenvalues are arranged from largest to smallest value. The elbow in the scree plot, or about 90% retention of the cumulative eigenvalues, can be taken as the cutoff for selecting significant principal components.[10]

ICA extends PCA by recovering statistically independent source signals from mixed observations, rather than merely orthogonal components maximizing variance. This advancement enables deeper insights into non-Gaussian data structures, such as blind source separation in multivariate signals. PCA utilizes the uncorrelatedness (second-order moment) criteria alone and hence cannot decode the hidden pattern in the original data. However, ICA transforms the original data into independent components by maximizing the non-Gaussian using the third-order moment.[11]

$$S = WX \quad \ldots (4)$$

where, X shows original sources, S represents the mixed signals, and W represents the mixing matrix.

$$X = AS \quad \ldots (5)$$

where, A is the unmixing matrix.

The ICA technique, widely recognized in the field, is a prominent algorithm utilized for addressing the cocktail party problem.[12] This problem revolves around the objective of discerning or isolating the auditory signals generated by individual sources, amidst the presence of multiple overlapping sounds within the surrounding environment.[12]

Materials and Methods

Data Acquisition

In the present N-back EEG study, a total of 21 subjects (8 females) participated. Following a comprehensive briefing on the study's procedures and objectives, written consent for participation was obtained from each individual. The participants' mean age was reported as 28 ± 6 years. Within this investigation, visual stimuli were presented to the subjects in the form of two distinct objects, namely a square and a circle, positioned at the corners of a computer screen. These objects were randomly relocated to occupy any of the four corners, resulting in six unique visual stimuli configurations. The subjects were instructed to respond whenever the spatial positions of the objects on the current screen matched those from the stimulus presented "n" steps earlier (n = 1, 2). Keypresses from a keypad were recorded to capture the subjects' responses. In the case of 0-back experiments, a specific pattern was designated, and subjects were directed to indicate its occurrence within the stimulus sequences. The stimuli, presented using the STIM2 system (Neuro-Scan) program, were randomized and presented consecutively, triggering corresponding codes in the EEG system. The inter-stimulus interval was kept at duration of 2 seconds. Each N-back experiment lasted 10 minutes, encompassing the presentation of 300 visual stimuli to the subjects. Following each experiment, a 10-minute break was provided to the participants. Brain signal acquisition was performed using a 64-channel Neuro-Scan EEG system, employing a sampling rate of 1 kHz and a bandwidth that extended from DC to 200 Hz. To facilitate analysis, the EEG data were segmented into epochs of 1800 ms, with the stimulus onset serving as the trigger point. A subset of EEG recorded segments exhibited severe artifacts and were therefore excluded from analysis when their absolute deviation exceeded 100 microvolts. Prior to conducting further analysis on the EEG data, measures were taken to eliminate biological artifacts, such as eyeblink and cardiac artifacts.[13]

Data Analysis

Classification Algorithms

Various Machine Learning (ML) models were employed to classify the N-back tasks using the Scikit-learn library in Python. The ML models considered in this study include:

i) K-Nearest Neighbour (k-NN): This model determines the classification of a new data point based on the majority class among its k-nearest neighbors.[14] Multiple values of k were tested, and through experimentation, it was determined that the optimal value of k was 5.

ii) Support Vector Machine (SVM): Using the radial basis function (RBF) kernel, the SVM maps the

input data into a higher-dimensional feature space. The optimal hyperplane, characterized by the maximum margin between different classes, is identified to achieve the best classification.[14]

iii) Multilayer Perceptron (MLP): The MLP model comprises multiple layers of perceptrons, combining a non-linear activation function with the back-propagation algorithm to search for the optimum classification. In this study, the hidden layers were configured with 50 neurons.[14]

iv) Random forest: This model operates through the training of multiple decision trees and reaches a final classification by employing an ensemble approach that utilizes the majority vote as the determining factor.

Training and Evaluation

a) K-fold cross-validation: The employed methodology involves partitioning the dataset into K distinct sections, wherein (K-1) sections are employed for training purposes, while one section is dedicated to testing. The significance of utilizing K-fold cross-validation lies in the fact that each section is utilized for testing, thereby ensuring a comprehensive evaluation. For this study, a value of K=10 was consistently selected across all machine learning models.

b) Accuracy, a widely adopted metric for evaluating classifier performance, is employed to compare the effectiveness of different classifiers. Classification accuracy quantifies model performance as the proportion of correctly predicted instances relative to the total dataset size. This metric evaluates overall classifier reliability by capturing the fraction of accurate predictions across all classes. It facilitates direct benchmarking of competing feature reduction and classification methods in EEG analysis.

Features Extraction

The multichannel EEG recordings were decomposed into multivariate intrinsic mode functions using MEMD. A segment of the multichannel EEG data decomposition, specifically depicting the decomposed data for the F1 channel, is shown in Fig. 2. After decomposing the data into IMFs, a set of 10 distinct features was extracted from each IMF. These features encompass the following:

i) Spectral-based features: Spectral power was determined using Welch's technique, wherein 50% of the data points were overlapped between consecutive windows. Power values were computed for spontaneous neural rhythms across the Delta (0–4 Hz), Theta (4–7 Hz), Alpha (7–13 Hz), Beta (13–30 Hz), and Gamma (30–80 Hz) frequency bands.[15]

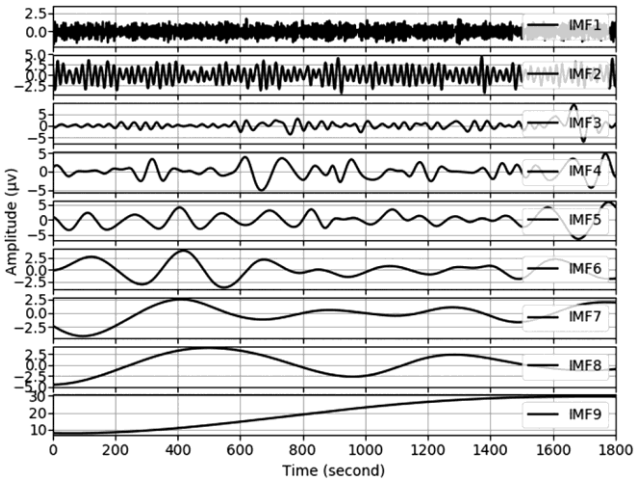

Fig. 2 — Intrinsic Mode Functions of the decomposed EEG data for the F1 channel

ii) Statistically based parameters: To characterize the signal of interest, various statistical properties were computed, including variance, absolute skewness, and kurtosis. By extracting these features, a comprehensive representation of the EEG data is obtained, capturing both spectral characteristics and statistical properties for further analysis and interpretation.

a) Variance: It is a statistical measure that quantifies the dispersion of data points relative to the mean. It helps researchers to gain valuable insights into the variability and distributional characteristics of the data, aiding in the understanding and analysis of the underlying phenomena or processes being investigated.

$$Variance = E\left[\left(x-\mu\right)^2\right] \quad \ldots (6)$$

where, E is the expectation operator, and μ is the mean.

b) Skewness: It provides a means to assess the degree of asymmetry exhibited by a distribution with respect to its mean value.[15] It measures the degree to which the distribution diverges from ideal symmetry. Positive skewness exhibits a longer tail on the right side of the distribution, indicating a relatively higher concentration of data points toward the left of the mean. The lateral shift against the normal distribution can be seen for an absolute value of skewness (abs_skew).

$$Skewness = E\left[\left\{\frac{x-\mu}{\sigma}\right\}^3\right] \quad \ldots (7)$$

where, σ is the standard deviation.

c) Kurtosis: It quantifies the degree of peakedness or the sharpness of the distribution of data points within a signal of interest.[15] The evaluation of kurtosis allows for the identification of potential non-Gaussian or non-normal behavior within the signal.

$$Kurtosis = \frac{\mu_4}{\sigma^4} \quad \ldots (8)$$

iii) Time-series-based parameters:

a) Zero crossing rate (zer cr): It quantifies the frequency of sign changes observed within a signal. It is widely utilized for analyzing non-stationary signals.[16]

b) Relative MEMD energy (RME): This metric is used to assess the relative distribution of energy across the various Intrinsic Mode Functions (IMFs) obtained through MEMD.

$$RME = \frac{Energy_k}{Energy_t} \quad \ldots (9)$$

where, $Energy_k$ is the energy at the kth IMF, while $Energy_t$ is the total energy.

Recent investigations have demonstrated that subdividing brain waves into narrower frequency bands yields a stronger correlation with cognitive tasks. Specifically, it has been observed that high-alpha power (10–13 Hz) exhibits an inverse relationship with cognitive tasks, whereas increased beta-band power (20–32 Hz) is linked to working memory.[17] In light of these findings, we employed Multiscale Empirical Mode Decomposition (MEMD) to partition brain waves into smaller subgroups based on frequency bands. The extracted features from the Intrinsic Mode Functions (IMFs), obtained through MEMD applied to EEG data, are presented in Table 1.

Each IMF yielded ten distinct features, resulting in a total of 5760 features per subject. This calculation was determined by multiplying the number of different features (10), the number of IMFs (9), and the number of EEG channels (64). Given that the number of features grows exponentially with the inclusion of 21 subjects, it becomes apparent that managing such a large volume of data becomes challenging. To mitigate this issue, a feature reduction approach was implemented to eliminate redundant information contained within the input features.

Results

In this work, the original feature set was transformed using Principal Component Analysis (PCA) to produce a new set of features that are statistically uncorrelated. The objective was to retain approximately 90% of the variances in all the classes, as illustrated in Fig. 3. The resulting uncorrelated

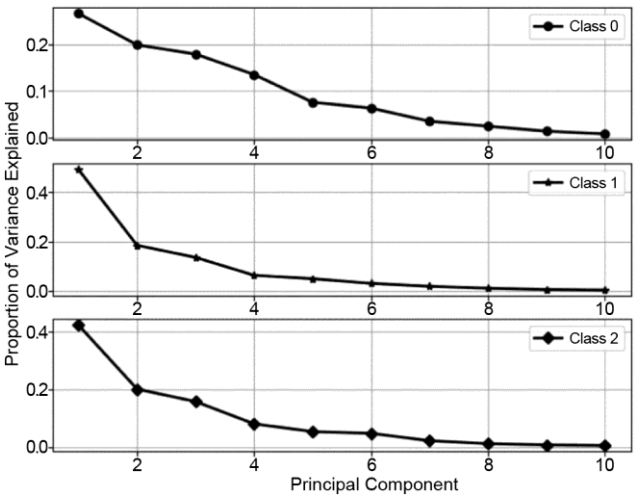

Fig. 3 — Identification and selection of significant principal components

Table 1 — Features extracted from each Intrinsic Mode Function corresponding to the frontal lobe channel (F1)

IMF	Delta- band	Theta- band	Alpha- band	Beta-band	Gamma- band	variance	abs skew	kurtosis	zer cr	RME
1	4.17E-05	7.29E-05	6.22E-05	4.89E-05	0.00034	0.47815	0.05694	−0.72691	541	0.00098
2	0.00037	0.001151	0.00166	0.00404	0.03503	2.77361	0.02553	−0.81665	181	0.0057339
3	0.0360	0.0296	0.0325	0.0714	0.0013	2.6595	1.0552	7.0532	87	0.00557
4	0.0260	0.2481	0.2115	0.0313	1.72E-05	2.9996	0.07128	0.4612	41	0.00620
5	0.0890	0.6394	0.0973	0.0025	3.28E-07	4.9839	0.0821	0.3008	28	0.0103
6	0.4434	0.0955	0.00063	5.56E-06	1.91E-09	2.6437	0.0209	−0.2092	14	0.00546
7	0.2260	0.0004	2.89E-06	1.02E-07	2.98E-10	2.4548	0.6766	0.2254	7	0.0051
8	0.2970	0.00074	2.07E-05	7.65E-07	2.30E-09	4.9861	0.0888	−0.9182	4	0.0103
9	0.2218	0.00107	4.71E-05	1.92E-06	6.22E-09	64.6770	0.2174	−1.5124	0	0.9502

Table 2 — Reduced transformed features obtained by applying PCA to the original 10 raw features

IMF	PC1	PC2	PC3	PC4	PC5
1	−1.0405	−1.26704	−1.5494	2.01868	0.9772
2	−1.6058	−0.44690	−1.3700	−1.3926	0.6039
3	−0.4388	0.160965	−0.5933	−1.3845	−0.728
4	−1.2911	−0.08586	−0.3348	−0.3981	0.0361
5	−1.3350	−1.39572	3.37663	0.36087	−0.665
6	−0.4362	3.647824	0.47814	1.49629	0.7441
7	3.39594	−0.44775	1.33681	−0.7867	1.2209
8	1.71239	−0.34494	−1.1782	1.06584	−1.461
9	−0.6837	−1.01320	−1.7422	1.81439	0.4156

Table 3 — Comparative analysis of classification performance using raw features versus PCA-reduced features

MLmodels	Avg. accuracy obtained using raw features	Avg. accuracy obtained using PCA transformed features
KNN	86.94%	91.89%
SVM	82.49%	86.59%
MLP	82.87%	91.04%
Random forest	86.86%	91.52%

Table 4 — Feature reduction was performed using ICA on a set of 10 raw features, resulting in 4 transformed features

IMF	IC1	IC2	IC3	IC4
1	0.02579	0.000731	−0.0105	0.03789
2	−0.0290	−0.00821	0.00539	0.02165
3	−0.0232	−0.00920	0.00661	0.00228
4	−0.0135	0.002808	−0.0039	0.01073
5	0.00201	0.055400	0.00503	−0.0112
6	0.00862	−0.00786	−0.0519	−0.0236
7	0.01126	−0.00361	0.03237	−0.0339
8	0.02650	−0.01843	0.00467	0.00629
9	0.02426	−0.00551	−0.0094	0.03476

Table 5 — Performance of classifications achieved by utilizing ICA on transformed features

ML models	Avg. accuracy obtained using ICA-derived features	Avg. precision obtained using ICA-derived features	Avg. recall obtained using ICA-derived features
KNN	95.26%	96.52%	94.35%
SVM	91.70%	92.80%	90.60%
MLP	93.60%	94.40%	92.90%
Random forest	93.82%	94.15%	93.20%

features obtained through PCA are presented in Table 2, demonstrating a 50% reduction in the number of features. Utilizing these uncorrelated features as input for the classifiers yielded enhanced performance, as indicated in Table 3.

However, it is crucial to go beyond the sole consideration of uncorrelatedness in the feature space, which solely relies on second-order statistics, in order to achieve effective feature reduction. Therefore, ICA was employed for feature reduction due to its reliance on third-order statistics. The selection of significant independent features using ICA was initialized based on PCA, and in this study, the optimal number of independent components was found to be 4.

The features extracted using ICA are presented in Table 4, whereas the classification outcomes obtained from the evaluated machine learning models are reported in Table 5. Among the considered classifiers, the KNN approach achieved the highest average classification accuracy of 95.26%. This performance was followed by the Random Forest, Multilayer Perceptron, and Support Vector Machine models, which attained accuracies of 93.82%, 93.60%, and 91.70%, respectively. A comparative analysis of Tables 3 and 5 indicates that the KNN classifier achieves optimal performance when the extracted features preserve statistical independence, underscoring the effectiveness of ICA-based feature representation.

Discussion

In this study, the MEMD technique is employed to analyze EEG data. This technique utilizes basis functions derived directly from the data itself, enabling a more comprehensive examination of the

Table 6 — Evaluation of the classification accuracy based on different techniques

Authors	*Features*	*Accuracy*
Mahmoud *et al*.[18], 2017	Discrete Wavelet Transform +stepwise regression	92.86%
Gupta *et al*.[19], 2020	Analytic wavelet transform	90.86%
Guan Kai, *et al*.[20], 2021	Ratio of power in Theta and Alpha band	73.25%
Duleme *et al*. [21], 2023	Ratio of power in alpha-/beta-band and delta-/theta-band	82.63%
Proposed approach	ICA based feature reduction	95.26%

underlying dynamics. Furthermore, effective feature reduction is achieved through the utilization of the independence property, leading to improved classification outcomes. It is important to highlight that the present work does not consider features based on evoked response potentials (ERPs). ERPs necessitate the averaging of numerous single-trial responses, obtained by repeatedly presenting similar trials (typically around 100 times). However, this approach may introduce the potential influence of mental fatigue on the EEG experiment.[17]

An ANOVA test is conducted to statistically quantify the results obtained from different techniques. The analysis reveals a statistically significant difference ($p<0.0006$) in classification accuracy among the various approaches. Furthermore, Tukey's Honestly Significant Difference (HSD) test indicates a significant difference ($p<0.05$) between the proposed approach and the other methods.

The efficacy of the current technique is assessed through a comparative analysis shown in Table 6. The performance of the current technique was validated against modern cognitive study methods using the data recorded during this investigation. Findings show that features transformed via ICA, which prioritize higher-order statistical independence, yield superior classification results. This approach effectively streamlines the feature set, proving that independence-based extraction is highly efficient for high-dimensional neural data.

Conclusions

This work presents an efficient EEG feature reduction framework that prioritizes statistical independence over standard feature decorrelation. By integrating ICA with a KNN classifier, the proposed method achieved a peak classification accuracy of 95.26%. Comparative analyses demonstrate that this framework significantly outperforms conventional approaches while maintaining low computational complexity, rendering it ideal for real-time processing of high-dimensional neural data. These results underscore the necessity of higher-order statistical feature extraction when dealing with non-stationary signals. Due to its robustness and efficiency, the proposed methodology offers a scalable solution for cognitive workload assessment and diverse biomedical signal analysis tasks. Future research will focus on hybrid strategies, specifically merging ICA with deep learning architectures to capture hierarchical and non-linear feature representations. Such advancements are poised to enhance classification reliability further and drive the evolution of next-generation diagnostic systems and brain–computer interface technologies.

Conflict of Interest

No potential conflicts of interest are there to be reported by the authors.

Ethical approval

All participants gave informed consent before the commencement of this study.

Acknowledgement

The authors thank the Director of MSG for their vital support during this research.

References

1 Iqbal M U, Shahab M A, Choudhary M, Srinivasan B & Srinivasan R, Electroencephalography (EEG) based cognitive measures for evaluating the effectiveness of operator training, *Process Saf Environ Prot*, **150** (2021) 51–67, doi:10.1016/j.psep.2021.03.048.

2 Mulert C, Simultaneous EEG and fMRI: Towards the characterization of structure and dynamics of brain networks, *Dialogues Clin Neurosci*, **15(3)** (2013) 381–386, doi: 10.31887/DCNS.2013.15.3/cmulert.

3 Zhou Y, Huang S, Xu Z, Wang P, Wu X & Zhang D, Cognitive workload recognition using EEG signals and machine learning- A review, IEEE *Trans Cogn Dev Syst*, **14(3)** (2022), 799–818, doi:10.1109/TCDS.2021.3090218.

4 Pergher V, Wittevrongel B, Tournoy J, Schoenmakers B & Van Hulle M M, Mental workload of young and older adults gauged with ERPs and spectral power during n-back task performance, *Biol Psychol*, **146** (2019) 107726, doi:10.1016/j.biopsycho.2019.04.004.

5 Labate D, Foresta F L, Occhiuto G, Morabito F C, Lay Ekuakille A & Vergallo P, Empirical mode decomposition vs. wavelet decomposition for the extraction of respiratory

signal from single-channel ECG: A comparison, *IEEE Sens J*, **13(7)** (2013) 2666–2674, doi:10.1109/JSEN.2013.2253316.

6 Abdullah S M U, Rehman N U, Khan M M & Mandic D P, A multivariate empirical mode decomposition-based approach to pansharpening, *IEEE Trans Geosci Remote Sens*, **53(7)** (2015) 3974–3984, doi:10.1109/TGRS.2014.2386687.

7 Patel R, Gireesan K, Baskaran R & Chandra Shekar N V, Optimal classification of N-back task EEG data by performing effective feature reduction, *Sadhana*, **47** (2022) 1–12, doi:10.1007/s12046-022-02015-w.

8 Murawwat S, Asif H M, Ijaz S, Imran Malik M & Raahemifar K, Denoising and classification of arrhythmia using MEMD and ANN, Alex *Eng J*, **61(4)** (2022) 2807–2823, doi:10.1016/j.aej.2021.08.014.

9 Berrich Y & Guennoun Z, EEG-based epilepsy detection using CNN-SVM and DNN-SVM with feature dimensionality reduction by PCA, S*ci Rep*, **15** (2025) 14313, doi:10.1038/s41598-025-95831-z.

10 Jolliffe I T & Cadima J, Principal component analysis: A review and recent developments, *Philos Trans A Math Phys Eng Sci*, **374** (2016) 21050202, doi:10.1098/rsta.2015.0202.

11 Smrdel A, Independent component analysis of oddball EEG recordings to detect Parkinson's disease, S*cientific Reports*, 15 (2025) 21889, doi:10.1038/s41598-025-07645-8.

12 Agrawal J, Gupta M & Garg H, A review on speech separation in cocktail party environment: Challenges and approaches, *Multimed Tools Appl*, **82** (2023) 31035–31067, doi:10.1007/s11042-023-14649-x.

13 Patel R, Gireesan K, Sengottuvel S, Janawadkar M P & Radhakrishnan T S, Common methodology for cardiac and ocular artifact suppression from EEG recordings by combining ensemble empirical mode decomposition with regression approach, *J Med Biol Eng*, **37** (2017) 201–208, doi:10.1007/s40846-016-0208-y.

14 Hosseini M P, Hosseini A & Ahi K, A review on machine learning for EEG signal processing in bioengineering, *IEEE Rev Biomed Eng*, **14** (2021) 204–218, doi:10.1109/RBME.2020.2969719.

15 Davis J J, Kozma R & Schubeler F, Analysis of meditation vs. sensory engaged brain states using shannon entropy and Pearson's first skewness coefficient extracted from EEG data, *Sensors*, **23** (2023) 1293, doi:10.3390/s23031293.

16 Xu H, Ebrahim M P, Hasan K, Heydari F, HowleyP & Yuce M R, Accurate heart rate and respiration rate detection based on a higher-order harmonics peak selection method using radar non-contact sensors, *Sensors*, **22(1)** (2022) 0083, doi:10.3390/s22010083.

17 Daume J, Graetz S, Gruber T, Engel A K & Friese U, Cognitive control during audiovisual working memory engages frontotemporal theta-band interactions, *Sci Rep*, **7** (2017) 12585, doi:10.1038/s41598-017-12511-3.

18 Mahmoud R, Shanableh T, Bodala I P, Thakor N V & Nashash H Al, Novel classification system for classifying cognitive workload levels under vague visual stimulation, IEEE *Sens J*, **17(21)** (2017) 7019–7028, doi:10.1109/JSEN.2017.2719460.

19 Gupta S S & Manthalkar R R, Classification of visual cognitive workload using analytic wavelet transform,*Biomed Signal Process Control*, **61**(2020), doi:10.1016/j.bspc.2020.101961.

20 Guan K, Chai X, Zhang Z, Li Q & Niu H, Evaluation of mental workload in working memory tasks with different information types based on EEG, *Proc Annu Int Conf* IEEE *Eng Med Biol Soc*, (2021) 5682–5685, 10.1109/EMBC46164.2021.9630575.

21 Duleme M, Perrey S & Dray G, Stable decoding of working memory load through frequency bands, *Cogn Neurosci*, **14(1)** (2022) 1–14, doi:10.1080/17588928.2022.2026312.